

# Morphology change of oxygen-restructured $\text{TiO}_2(110)$ surfaces by UHV annealing: Formation of a low-temperature $(1 \times 2)$ structure

Min Li, Wilhelm Hebenstreit, and Ulrike Diebold\*

*Department of Physics, Tulane University, New Orleans, Louisiana 70118*

(Received 6 July 1999)

When reduced  $\text{TiO}_2(110)$  single crystals are oxidized at moderate temperatures (470–660 K), the surfaces restructure. Interstitial Ti atoms from the bulk diffuse to the surface where they react with gaseous oxygen and form new, added  $\text{TiO}_2$  layers. These are characterized by three structural elements: small  $(1 \times 1)$  islands, irregular networks of pseudohexagonal rosettes, and  $[001]$ -oriented strands. The strands exhibit the same structural characteristics as the  $(1 \times 2)$  surface reconstruction, which forms upon annealing at higher temperatures. Atomic-resolution scanning tunneling microscopy images of the strands are consistent with the added- $\text{Ti}_2\text{O}_3$ -row model. UHV annealing of oxygen-restructured surfaces smooths the surfaces and converts the rosette networks into strands and finally into regular  $(1 \times 1)$  terraces. The composition of these oxygen-induced phases is quantified using  $^{18}\text{O}_2$  gas in combination with low-energy  $\text{He}^+$  ion scattering measurements. Dynamic processes for the conversion from rosette networks into  $(1 \times 2)$  strands and ultimately into  $(1 \times 1)$  terraces are discussed.

## I. INTRODUCTION

### A. Motivation

The  $\text{TiO}_2(110)$  surface has become the most popular system for surface-science investigations of metal oxides in recent years. The different structures and morphologies that evolve during sample preparation are therefore of considerable interest. It is well established by experiment<sup>1–3</sup> as well as theory<sup>4</sup> that the  $(1 \times 1)$  surface is bulk-terminated with some relaxations, while the atomic structure and stability range of the  $(1 \times 2)$  reconstruction is still subject to debate (see below). Our own interest in the  $(1 \times 2)$  structure has been stimulated by our recent observation of a massive restructuring process that takes place upon reoxidizing reduced  $\text{TiO}_2$  single crystals at moderate temperatures.

We found that annealing flat,  $(1 \times 1)$ -terminated  $\text{TiO}_2(110)$  surfaces in moderate oxygen pressures changes the surface morphology and structure substantially.<sup>5–7</sup> A formation mechanism involving the reaction of interstitial Ti atoms (diffusing from the reduced bulk to the surface) with oxygen offered from the gas phase was confirmed by low-energy ion scattering (LEIS) experiments using isotopically labeled  $^{18}\text{O}_2$ . Restructured surfaces are quite rough and dominated by three small-scale features: irregular networks of connected,  $6 \times 6.5$ -Å-wide rosettes; one-unit-cell-wide  $[001]$ -oriented strands [with an appearance in scanning tunneling microscopy (STM) images similar to the  $(1 \times 2)$  reconstruction]; and small (tens of Å)  $(1 \times 1)$  islands (see Fig. 1). The formation and stability range of these structures depend on a variety of preparation parameters, such as oxygen pressure, annealing temperature, annealing time, and reduction state of the crystal.<sup>7</sup> We have proposed that the rosettes consist of an incomplete  $\text{TiO}_2$  layer with atoms missing in a regular fashion. First-principles calculations have shown that these are stable structures.<sup>7</sup>

In this paper, we focus on the atomic structure of the  $(1 \times 2)$  strands as well as the thermal stability of all three

structural elements. Restructured surfaces are annealed in ultrahigh vacuum (UHV) at temperatures between 620 and 830 K. The surface morphology after annealing is monitored with STM, and the surface concentration of  $^{18}\text{O}$  surfaces is quantified with LEIS. Rosette networks disappear quickly and convert partially into  $(1 \times 2)$  strands. This “low-temperature”  $(1 \times 2)$  phase is converted into flat  $(1 \times 1)$ -terminated terraces surfaces through UHV annealing at 830 K.

### B. The $(1 \times 2)$ structure

Because the atomic structure of the  $(1 \times 2)$  phase is under detailed discussion, we give a brief survey of the current state of knowledge and the proposed structural models.

A  $(1 \times 2)$  low-energy electron diffraction (LEED) pattern was originally observed after high-temperature annealing of a reduced  $\text{TiO}_2(110)$  sample in UHV. It was interpreted as alternate rows of bridging oxygen missing from the regular  $(1 \times 1)$  surface (“missing-row model”<sup>8</sup>). A variety of STM images of this surface reconstruction were published by different groups.<sup>9–16</sup> Bright strands running along the substrate  $[001]$  direction with a minimum separation of 13 Å were observed. The  $(1 \times 2)$  reconstruction appears to be stable in a relatively wide temperature range, and higher periodicities, i.e., a local  $(1 \times 3)$  reconstruction, have also been observed.<sup>13,17</sup> In addition, many researchers report scattered single bright strings on a  $(1 \times 1)$  surface prepared by annealing in UHV to lower temperatures. These are located at the same position and have an appearance similar to the  $(1 \times 2)$  strands.<sup>6,9,12,13,18,19</sup> Some but not all groups report a cross-linking of the  $(1 \times 2)$  rows along the  $[1\bar{1}0]$  direction.<sup>11,12,16,20,21</sup> Engel and co-workers reported the first STM images after annealing the surface in  $\text{O}_2$ , and observed pronounced cross-linking with local  $c(2 \times 1)$  units after re-annealing the oxygen-treated surface in UHV.<sup>11,21</sup> More recently, the structure of these cross-links has been resolved in high-temperature STM images.<sup>16,20</sup>

The  $(1 \times 2)$  strands are generally observed to have a height smaller than a regular  $\text{TiO}_2$  step edge of  $3.2 \text{ \AA}$  and to be in registry with the bright rows of the  $(1 \times 1)$  substrate. Because most researchers report empty-state images and because these are dominated by the tunneling into mostly  $\text{Ti } 3d$ -derived states,<sup>22</sup> bright strands centered on top of bright substrate rows imply that the  $(1 \times 2)$  strands are at the position of fivefold-coordinated Ti atoms and not at the bridging oxygen atoms. This discounts a simple missing-row model. Because most of the  $(1 \times 2)$  rows extend out of step edges, a modified model has been proposed by Murray, Condon, and Thornton,<sup>12</sup> which involves narrow rows with missing bridging oxygens that are effectively part of the upper terrace. Lateral relaxations were also included.<sup>12,21</sup> This model was shown to be consistent with calculated surface charge densities.<sup>23</sup> Early on, Onishi and Iwasawa<sup>10</sup> suggested a quite different model. It consists of strings with  $\text{Ti}_2\text{O}_3$  stoichiometry, consisting of double rows of Ti cations at (normally empty) octahedral positions, surrounded by oxygen atoms. Self-consistent total-energy and electronic structure calculation found that this added- $\text{Ti}_2\text{O}_3$ -row structure has a lower surface free energy than the missing-row structure.<sup>24</sup> It is also supported by ESDIAD (Ref. 25) as well as more recent STM measurements.<sup>15</sup>

Recently, a different added-row model has been proposed by Pang *et al.*<sup>17</sup> In this model, all atoms are in bulklike positions, and all the bridging oxygen atoms are missing, resulting in an overall  $\text{Ti}_3\text{O}_5$  stoichiometry. In addition, the Ti atoms underneath some of the bridging oxygen rows are removed, which gives rise to the dark regions separating the bright ridges in the  $(1 \times 2)$  structure. The missing units are similar to a proposal made by Fischer *et al.*<sup>18</sup> to explain the bright  $(1 \times 2)$  strands on the  $(1 \times 1)$  surface.

The thermal stability range, formation mechanism of the  $(1 \times 2)$  phase, and the role of gaseous oxygen in this process are still unclear. While most researchers produced the  $(1 \times 2)$  reconstruction through UHV annealing at high temperatures ( $\geq 1000 \text{ K}$ ), Xu *et al.* report a  $(1 \times 2)$  phase with a very similar appearance can also be formed by annealing at low temperature ( $700\text{--}800 \text{ K}$ ).<sup>14</sup> At somewhat higher temperatures, it converts to the  $(1 \times 1)$  surface. To date, two groups have studied the formation of the  $(1 \times 2)$  phase using STM measurements at elevated temperatures.<sup>16,20,26</sup> Onishi and Iwasawa report the formation of  $(1 \times 2)$  strands while keeping the sample at  $800 \text{ K}$  in an oxygen background pressure of  $1 \times 10^{-7} \text{ mbar}$ . These strands were interpreted as added  $\text{Ti}_2\text{O}_3$  rows. Very recent STM images taken at  $873 \text{ K}$  in  $5.5 \times 10^{-7} \text{ mbar}$  oxygen showed evidence for two different reconstructions, depending on the reduction state of the  $\text{TiO}_2$  crystal.<sup>16,20</sup> Added  $\text{Ti}_2\text{O}_3$  rows were formed on a more stoichiometric crystal, and a cross-linked  $(1 \times 2)$  structure was observed on more bulk reduced, darker  $\text{TiO}_2$  crystals. The cross-linked  $(1 \times 2)$  strands exhibit the same step height as the  $(1 \times 1)$  terminated surface, and were essentially interpreted as long lines of intact  $(1 \times 1)$  structure, separated by troughs of missing atoms. This is structurally similar to the Pang *et al.* model<sup>17</sup> with the addition of bridging oxygen atoms. The cross links have some resemblance to the rosettes observed in our previous work.<sup>7</sup> The cross-linked  $(1 \times 2)$  strands grow through reaction of interstitial Ti atoms with gaseous oxygen and are precursors to the growth of added

$(1 \times 1)$  layers.<sup>20</sup> The restructuring process was recorded by high-temperature STM movies<sup>20</sup> and was shown to occur through nucleation of cross-links strands at temperatures  $> 673 \text{ K}$ .

As shown in this work, the  $(1 \times 2)$  strands that appear upon annealing in oxygen at low temperature [ $< 660 \text{ K}$  (Ref. 7)] have a structure consistent with the Onishi-Iwasawa model. These strands are thermally more stable than rosette networks and develop a cross-linked appearance upon annealing in UHV. As will be shown in a forthcoming paper, the reduction state of the sample affects whether or not such strands are observed on sputtered and UHV-annealed  $(1 \times 1)$  surfaces.<sup>19</sup>

## II. EXPERIMENT

The experiments were conducted in a UHV system,<sup>7,27</sup> which is equipped with x-ray photoelectron spectroscopy (XPS), low-energy  $\text{He}^+$ -ion scattering spectroscopy (LEIS), LEED, and STM operating at room temperature. Two polished  $\text{TiO}_2$  single crystals have been used (Commercial Crystal Laboratories). Both samples exhibited a blue color after an initial high-temperature anneal ( $950 \text{ K}$ ). Sample mounting and treatment are described in Refs. 7 and 27. In order to monitor the oxygen incorporation during annealing excursions, isotopically enriched  $^{18}\text{O}_2$  gas ( $^{18}\text{O}_2 : ^{16}\text{O}_2 = 93\% : 7\%$ ) was employed. LEIS spectra show clearly resolved  $^{16}\text{O}$  and  $^{18}\text{O}$  peaks.<sup>7</sup> For quantification of the  $^{18}\text{O}$  surface content, these peaks were fitted with two Gaussians with equal widths after subtraction of a linear background, and the total peak area was normalized to 100%. LEIS measurements do not affect the uptake of  $^{18}\text{O}$  with carefully controlled parameters (total ion fluence of  $\sim 1.6 \times 10^{-15} \text{ cm}^{-2}$  per measurement and beam energy of  $1225 \text{ eV}$ ). The roughness of surfaces is quantified with the root-mean-square (rms) value of STM images. The rms roughness value is determined on the differentiated instead of the original STM images (Figs. 4 and 5) in order to emphasize the newly added features such as rosette network patches,  $(1 \times 2)$  strands, and  $\text{TiO}_2$  clusters, as well as step edges of  $(1 \times 1)$  islands. The rms roughness value presented in the results section is averaged over several images with similar quality. An error of  $0.2 \text{ \AA}$  is estimated for Figs. 4(a) and 4(b), and  $0.1 \text{ \AA}$  for Figs. 5(a)–5(d).

## III. RESULTS

The starting point for our experiments was restructured surfaces similar to the one shown in Fig. 1. These surfaces have been produced by reannealing in oxygen flat,  $(1 \times 1)$ -terminated  $\text{TiO}_2(110)$  crystals (which, in turn, have been obtained through  $\text{Ar}^+$  sputtering and annealing in UHV at  $880 \text{ K}$ ). Figure 1 shows pseudo-hexagonal rosettes (labeled *R* in Fig. 1), small  $(1 \times 1)$  islands, and short strands (with white features at both ends) that are typically present on such “restructured” surfaces. As seen in Fig. 1, and more clearly in the small-scale image of Fig. 2, most rosettes consist of six bright spots, which are considered Ti atoms. Atomic models for the rosettes have been presented before,<sup>5,7</sup> and rosettes connected to  $(1 \times 2)$  strands are depicted in Fig. 3. They consist of Ti and O atoms in bulklike positions, with

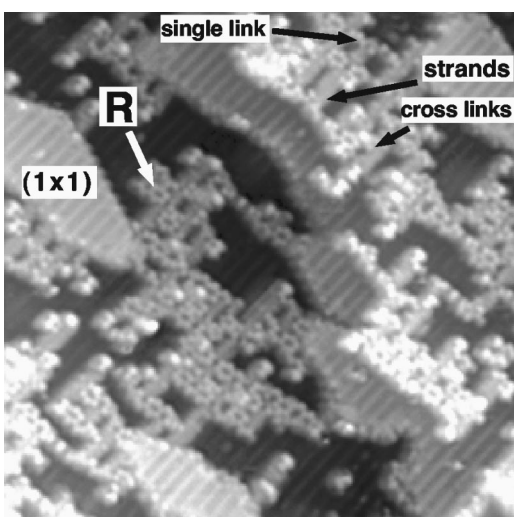


FIG. 1. STM image ( $300 \text{ \AA} \times 300 \text{ \AA}$ ) of a  $\text{TiO}_2(110)$  surface annealed in  $\text{O}_2$  ( $1 \times 10^{-6}$  mbar, 550 K, 20 min). Reoxidation of the reduced bulk causes formation of irregular networks of pseudo-hexagonal rosettes ( $R$ ), added small  $(1 \times 1)$  islands, and strands.

some atoms missing in a regular fashion. For example, adding one  $\text{TiO}_2$  unit into the center of a rosette would render a small island with  $(1 \times 1)$  structure. First-principles total-energy and electronic structure calculations predict that these rosettes are essentially stable structures and undergo substantial relaxations (ranging up to  $0.5 \text{ \AA}$ ).<sup>7</sup>

A similar “rosette” structure reported to exist on the  $(1 \times 2)$  reconstructed surface exhibits a range of cross-linked

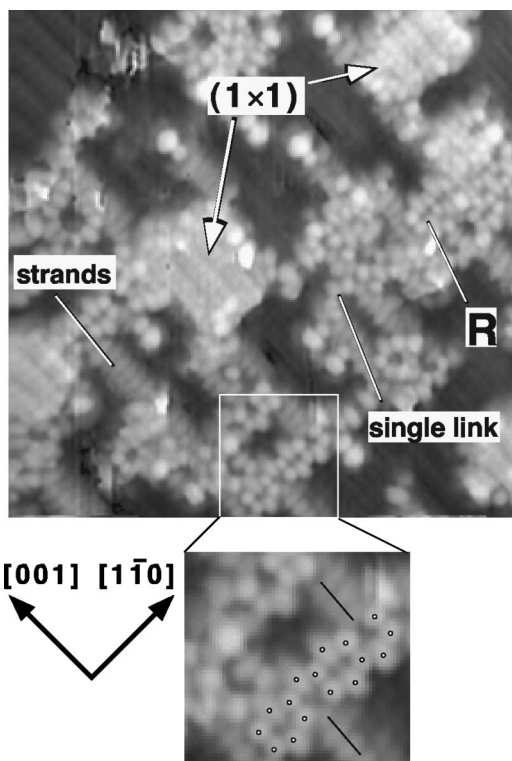


FIG. 2. Small-scale STM image ( $150 \text{ \AA} \times 150 \text{ \AA}$ ) of a reconstructed  $\text{TiO}_2(110)$  surface annealed in  $\text{O}_2$  ( $1 \times 10^{-6}$  mbar, 570 K, 25 min). Regular rosettes consist of six bright spots. Rosettes connected to strands miss the bright spot at the apex next to the strand.

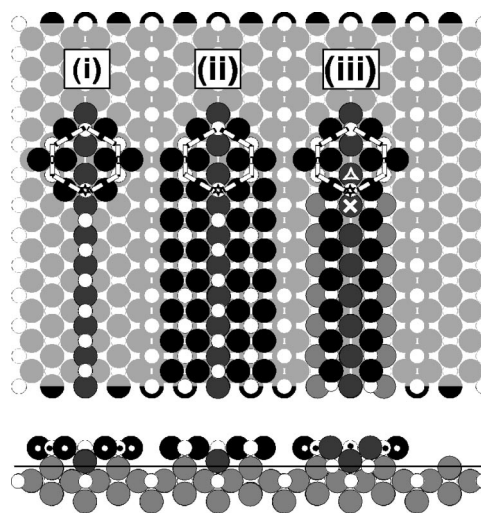


FIG. 3. Structural models for strands (top and side view) connected to rosettes. (i) The single Ti-O chain model (Ref. 5); (ii) the added- $\text{Ti}_3\text{O}_5$ -row model (Ref. 17); (iii) the added- $\text{Ti}_2\text{O}_3$ -row model (Refs. 10, 26, 28). Large black balls and small white balls correspond to oxygen and titanium atoms, respectively. Atoms belonging to rosettes are marked with dots in the side view.

structures.<sup>16,20</sup> The cross-linked structures include the single link and double links in the form of cross shapes, which are also visible in our STM images (Figs. 1, 2, and 6). In Ref. 16, a model was suggested for the cross-links, which resembles part of the rosette network depicted in Ref. 7 [Fig. 12(b)].

The bright strands in Figs. 1, 2, and 6 are in registry with the bright rows (with fivefold-coordinated Ti atoms) of the  $\text{TiO}_2(110)$  substrate, as is the case for the rows of the  $(1 \times 2)$  structure. Interestingly, rosettes always miss a bright atom (a Ti atom) when connected to a bright strand. This is exemplified in the inset of Fig. 2. In Fig. 3, we have drawn the established model for the rosettes together with three different possibilities for the  $(1 \times 2)$  strands: (i) an added-TiO model initially proposed by our group,<sup>5</sup> (ii)  $\text{Ti}_3\text{O}_5$  strands,<sup>17</sup> and (iii)  $\text{Ti}_2\text{O}_3$  strands.<sup>10,26,28</sup> In all three cases, the atom missing in the experimental image (Fig. 2) is marked by a star in the model. The implications of this observation are discussed in Sec. IV A.

Annealing reconstructed surfaces in UHV leads to an overall smoothing of the surfaces (Fig. 4). The starting point for Fig. 4 is a  $\text{Ti}^{18}\text{O}_2(110)$  surface prepared by 5 min  $^{18}\text{O}_2$  ( $1 \times 10^{-6}$  mbar) exposure at 660 K [Fig. 4(a)]. The  $1000 \text{ \AA} \times 1000 \text{ \AA}$ -wide image in Fig. 4(a) exhibits more than seven layers, and the  $(1 \times 1)$  step edges are irregularly shaped. The rms roughness value is  $1.4 \text{ \AA}$ . Annealing such a surface in UHV at 620 K for 2 min leads to a flatter surface (rms roughness value =  $1.1 \text{ \AA}$ ) with less than three layers exposed in Fig. 4(b) and smoother step edges of the main  $(1 \times 1)$  terraces. The added  $(1 \times 1)$  islands and rosette patches  $R$  are still visible in Fig. 4(b).

A more detailed UHV annealing study begins with a  $\text{Ti}^{18}\text{O}_2(110)$  surface annealed in  $^{18}\text{O}_2$  ( $1 \times 10^{-6}$  mbar) at 550 K for 10 min as shown in Fig. 5(a). After 2 min UHV anneal at 690 K [Fig. 5(b)], the network patches have partially disappeared and small  $(1 \times 1)$  islands dominate the image. Many isolated short strands ( $\sim 50 \text{ \AA}$  long) populate the

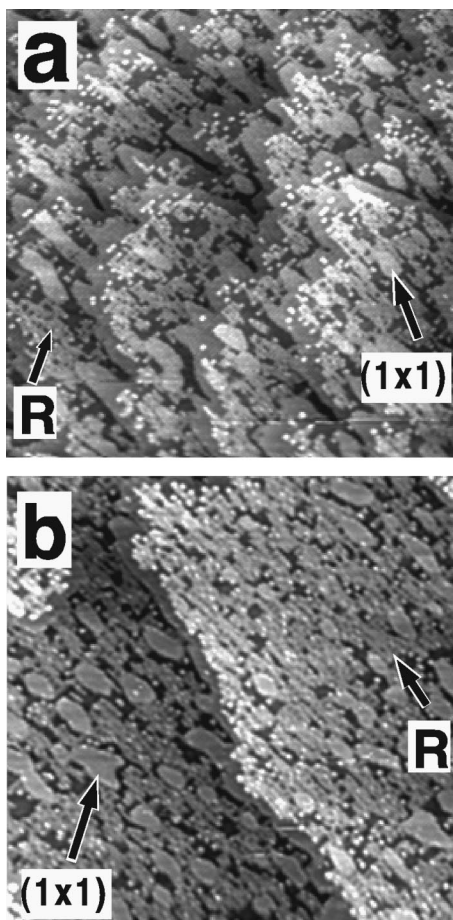


FIG. 4. STM images ( $1000 \text{ \AA} \times 1000 \text{ \AA}$ ) of a  $\text{Ti}^{18}\text{O}_2(110)$  surface: (a) after annealing in  $^{18}\text{O}_2$  for 5 min at 660 K, rms roughness value =  $1.4 \text{ \AA}$ , (b) followed by 2 min UHV anneal at 620 K, rms roughness value =  $1.1 \text{ \AA}$ .

$(1 \times 1)$  islands. A small-scale STM image (Fig. 6) shows that the network patches are now composed of  $[001]$ -oriented strands (ca.  $30 \text{ \AA}$  long) interconnected by a single chain of rosettes or  $[1\bar{1}0]$ -oriented rows. The closest distance between strands is  $13 \text{ \AA}$ , which is twice the width of the  $(1 \times 1)$  unit cell in the  $[1\bar{1}0]$  direction. The bright spots at both ends of the strands in Figs. 5(b) and 6 are commonly observed for the  $(1 \times 2)$  reconstruction.<sup>9,10</sup>

Continuing to anneal in UHV for 2 min at 780 K [Fig. 5(c)] flattens the surface further. Only a few isolated  $(1 \times 1)$  islands ( $70 \text{ \AA} \times 40 \text{ \AA}$ – $250 \text{ \AA} \times 100 \text{ \AA}$ ) can be seen while most of the  $(1 \times 1)$  islands become incorporated into step edges. This merging of smaller islands may have led to irregular holes distributed on the large flat terraces. The network patches have disappeared. Short strands (ca.  $50 \text{ \AA}$ ) are still visible, albeit their number decreases considerably. Further annealing in UHV for 2 min at 830 K [Fig. 5(d)] yields a surface that is similar to the UHV annealed surface. The step edges become smoother with very few  $[1\bar{1}0]$  elongated  $(1 \times 1)$  islands (typically  $160 \text{ \AA} \times 70 \text{ \AA}$ ) as extensions. No isolated  $(1 \times 1)$  islands exist. The irregular holes can still be seen on the terrace. The number of short strands with white ends is drastically decreased. The overall flattening of the surface is reflected in the decrease of rms roughness values from  $1.4 \text{ \AA}$  [Fig. 5(a)] to  $0.9 \text{ \AA}$  [Fig. 5(d)].

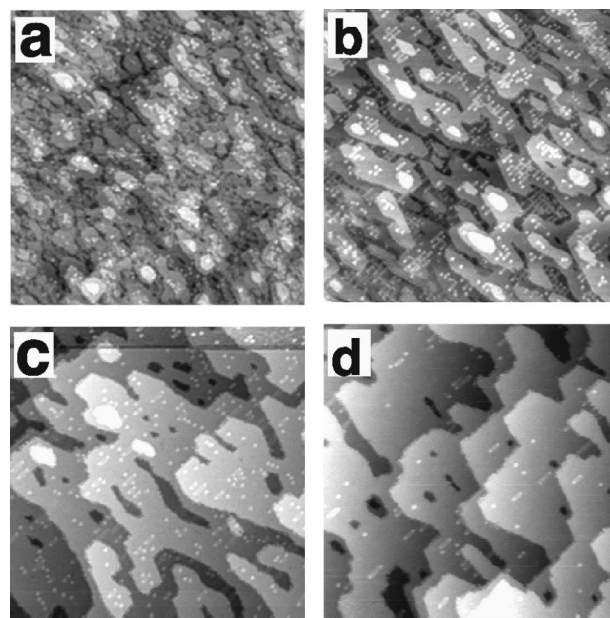


FIG. 5. STM images ( $1000 \text{ \AA} \times 1000 \text{ \AA}$ ) of  $\text{TiO}_2(110)$  surfaces: (a) 550 K annealing in  $1 \times 10^{-6}$  mbar  $^{18}\text{O}_2$  for 10 min, rms roughness value =  $1.4 \text{ \AA}$ ; and reannealing for 2 min in UHV at (b) 690 K, rms roughness value =  $1.2 \text{ \AA}$ , (c) 780 K, rms roughness value =  $1.1 \text{ \AA}$ , (d) 830 K, rms roughness value =  $0.9 \text{ \AA}$ .

A series of LEIS measurements was performed while keeping a  $\text{Ti}^{18}\text{O}_2(110)$  surface at elevated temperature in UHV. The surface was initially prepared by exposure to  $1 \times 10^{-6}$  mbar  $^{18}\text{O}_2$  at 500 K for 60 min. The temperature was stepped from 500 to 970 K; each temperature was kept for 5 min. The  $^{18}\text{O}$  surface content decreases from 40% at 500 K to 4% at 970 K during the experimental time (50 min) as shown in Fig. 7. After employing linear regressions through the data points, a turning point in the slope is found at 740 K. Below 740 K (region I), the  $^{18}\text{O}$  content drops with a rate of  $0.06 \text{ K}^{-1}$  and slides down much faster with a rate of  $\sim 0.1 \text{ K}^{-1}$  above 740 K (region II).

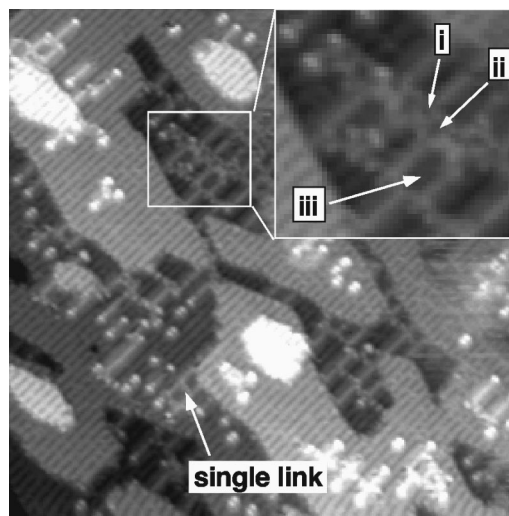


FIG. 6. STM image ( $500 \text{ \AA} \times 500 \text{ \AA}$ ) of a  $\text{TiO}_2(110)$  sample prepared as in Fig. 5(b). Labels (i)–(iii) in the inset refer to the atomic model in Fig. 8.

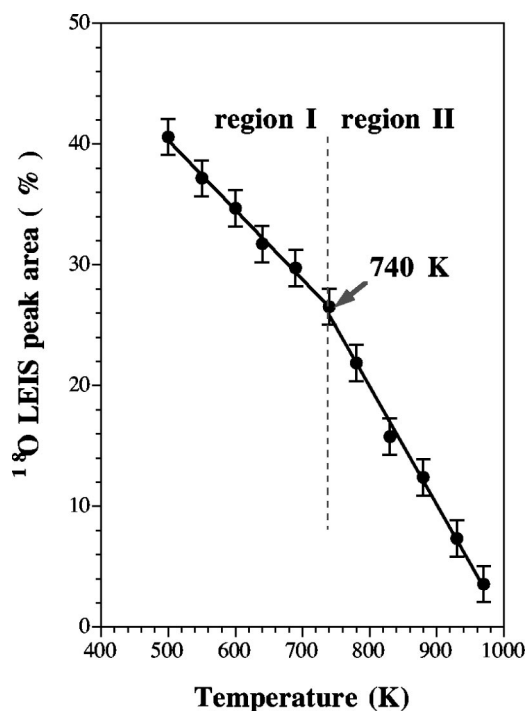


FIG. 7. Surface concentration of  $^{18}\text{O}$  determined from  $\text{He}^+$  LEIS peak areas during annealing in UHV at increasing temperatures (pretreatment: 60 min in  $^{18}\text{O}_2$ :  $1 \times 10^{-6}$  mbar at 500 K).

#### IV. DISCUSSION

##### A. Geometric model for strands

Bright strands with a similar appearance are visible on both oxygen-annealed  $\text{TiO}_2(110)$  surfaces [Figs. 1 and 2, strands connected to rosettes or  $(1 \times 1)$  islands] and UHV-annealed  $\text{Ti}^{18}\text{O}_2(110)$  surfaces [Figs. 5(b)–5(d) and 6]. These strands are located above bright rows of the  $(1 \times 1)$  substrate, at the position of fivefold-coordinated Ti atoms. They closely resemble the strands observed on  $(1 \times 2)$  surfaces that are formed upon annealing either in UHV (Refs. 9, 11–16, 18, 21, 26, and 28) or in oxygen ( $\sim 10^{-7}$  mbar) at 800 K.<sup>26</sup> In the atomically resolved STM image in Fig. 2, strands are composed of bright features with a separation of  $\sim 3$  Å along the  $[001]$  direction. It has been proposed that the white feature at ends of the strands (in our images most clearly observed on UHV-annealed surfaces, Fig. 6) corresponds to an increase in the local density of states (LDOS) for the atoms with reduced coordination number at the strand end.<sup>9,10</sup>

Why would such strands coexist with the rosette network? As shown in Figs. 1 and 2, the rosette networks and the added small  $(1 \times 1)$  islands are elongated along the  $[1\bar{1}0]$  direction, perpendicular to the surface  $[001]$  rows. As discussed in a previous paper,<sup>7</sup> connecting rosette units in the  $[1\bar{1}0]$  direction produces a slightly smaller Ti:O ratio than ideal stoichiometry (Ti:O = 1:2), leading to oxygen-rich surfaces. Possibly, this is the physical reason for the formation of strands composed of some form of substoichiometric titanium oxide. This way, the overall stoichiometry of the incomplete layer (composed of network patches and strands) should be close to Ti:O = 1:2.

Three possible geometrical models for strands connected to a single rosette are shown in Fig. 3. We use the models for strands that have been outlined in Sec. IB<sup>5,10,17,26,28</sup> and compare their expected appearance in STM images with our experimental observations (Fig. 2). The center of the strands must be aligned with the center of a rosette; they must have a periodicity of 3 Å along  $[001]$ ; they must appear lower than the rosette network in STM images; their stoichiometry must be  $\text{TiO}_x$  ( $x < 2$ ); and there should be a reason why the Ti atom of the lower apex of the rosette (marked with a star in Fig. 3) is always missing.

In a previous paper, we have proposed a single chain model as part of oxygen-restructured surfaces.<sup>5</sup> On top of a regular  $(1 \times 1)$  surface, Fig. 3(i) shows a structure consisting of twofold-coordinated Ti atoms supported by threefold-coordinated O atoms. The overall stoichiometry of such a strand is TiO in one unit cell as shown in Fig. 3(i). The Ti-O chain, aligned with the center of the rosette, is located on a row of fivefold-coordinated Ti atoms on the  $(1 \times 1)$  substrate. The broad ( $\sim 7.5$  Å in the  $[1\bar{1}0]$  direction) and lower (than rosette Ti atoms) appearance of strands has been attributed to the instability of a single Ti-O row structure, relaxations, and tip effects in our previous paper.<sup>5</sup> As pointed out above (inset in Fig. 2), a fourfold-coordinated Ti atom in the rosette (or two Ti atoms if the strands extend from both apices of the rosette) is always missing at the connection to the strand in our STM results. Such a Ti atom is marked by a star in Fig. 3. It is not immediately obvious why such an atom should be missing in the single-chain model, and we revoke our assignment made in Ref. 5.

Figure 3(ii) shows the model proposed in a recent paper by Pang *et al.*<sup>17</sup> Similar to the rosettes (Fig. 3, top part), it consists only of atoms in their bulklike positions. Fourfold-coordinated Ti atoms (two bridging O atoms are missing per Ti atom) are aligned with the rosette center. The row is terminated by twofold-coordinated in-plane O atoms on both sides, and the stoichiometry reaches Ti:O = 3:5 ( $\text{Ti}_3\text{O}_5$ ); which again may reduce the overall stoichiometry of rosettes and strands to Ti:O = 1:2. The strands observed by STM in Ref. 17 are composed of paired rows running along the  $[001]$  direction with a height of 2.5 Å; such a pairing is not resolved in our STM images. The separation of these features is  $\sim 3$  Å in the  $[001]$  direction, which agrees with our measurement. The distance between paired rows in the  $[1\bar{1}0]$  direction is  $\sim 5.5$  Å, close to the full width at half maximum of our strands. A good agreement was reached between STM results and first-principles atomic orbital based calculations based upon the proposed model in Ref. 17. Nevertheless, this model does not reflect well the relationship between rosettes and strands observed in our STM images (Figs. 1 and 2 and STM images in previous papers<sup>5,7</sup>). The strands of Pang *et al.* and the rosette network have a very similar geometric structure, and predicted relaxations collapse the rosettes somewhat inward.<sup>7</sup> Hence one would expect a similar width and height of the rosettes and the  $(1 \times 2)$  strand. In the experiment the strands appear narrower and lower than the rosettes. Most importantly, there is no particular reason why the marked Ti atom should disappear.

Finally, the added- $\text{Ti}_2\text{O}_3$ -row model of Onishi and Iwasawa is presented in Fig. 3(iii).<sup>10,26,28</sup> Two sixfold-coordinated Ti rows are located next to the threefold-

coordinated O atoms. These in turn are aligned with the center of the rosette and are located on top of the fivefold-coordinated Ti atoms of the substrate. These  $\text{Ti}^{3+}$  atoms are at the same octahedral position as interstitial Ti atoms in the bulk.<sup>29</sup> The stoichiometry is  $\text{Ti}:\text{O}=2:3$ , satisfying the need for a reduced  $\text{TiO}_x$  ( $x < 2$ ) feature coexistent with the rosette network. The added- $\text{Ti}_2\text{O}_3$  model is supported by STM studies of a DCOO-covered  $\text{TiO}_2(110)$  surface,<sup>28</sup> an ESDIAD study of  $(1 \times 2)$  reconstructed  $\text{TiO}_2(110)$  surface by Guo, Cocks, and Williams,<sup>25</sup> as well as Ng and Vanderbilt's calculations.<sup>24</sup> More recently, Tanner, Castell, and Briggs<sup>15</sup> reported STM results that also favored the  $\text{Ti}_2\text{O}_3$  model. The calculated near-conduction-band-minimum charge density of states exhibits a sharp increase around the position of the added  $\text{Ti}_2\text{O}_3$  units and the corrugation is about 1.5–2.0 Å, which is slightly larger than that of our strands (0.8 Å). Onishi and Iwasawa observed strands<sup>26</sup> composed of two ridges (2 Å high) separated by 3.5 Å; such a double structure is not resolved in our images. Note that the marked fourfold-coordinated Ti atom of the rosette together with the supporting O atom inside the rosette (marked with a triangle) has to be removed, otherwise the supporting O atom (marked with a cross) would become fourfold coordinated. All O atoms in the bulk rutile structure are threefold coordinated, and it is highly unlikely that a fourfold coordinated O atom should appear on the surface. These considerations correlate well with the missing atoms in our observed strands (Fig. 2).

Overall, while we cannot give conclusive evidence for either model, the Onishi-Iwasawa added- $\text{Ti}_2\text{O}_3$ -row model is most favored by our STM measurements. The difference of the strand height and width is within a range that could easily result from the changes in LDOS on the strands and through convolution with the tip during the scanning process. The most convincing evidence is the Ti atom that is missing at the apex of the rosette connected to the strand (Figs. 2 and 3). This is predicted to be missing in a  $\text{Ti}_2\text{O}_3$  strand connected to a rosette.

### B. Geometric model for cross-linked strands

As seen in the annealing series of Fig. 5, cross-linked  $(1 \times 2)$  strands are the precursors to the single strands observed at higher temperature. The inset in Fig. 6 shows an enlarged STM image of a  $\text{Ti}^{18}\text{O}_2$  surface, reannealed in UHV. Along the  $[1\bar{1}0]$  direction, a combination of single rosettes [(i),  $6.5 \text{ \AA} \times 6 \text{ \AA}$ ] and rings [(ii),  $6.5 \text{ \AA} \times 12 \text{ \AA}$ ] is observed with the typical order i-ii-i-ii-i-ii. Strands extend from either one or both ends of rosettes and rings. The strands themselves form the edges of larger rings [(iii),  $13 \text{ \AA} \times 23 \text{ \AA}$ ]. Based upon the Onishi-Iwasawa added- $\text{Ti}_2\text{O}_3$ -row model, an atomic model for a structure consisting of the three elements [the rosette (i), the ring (ii), and the large ring (iii)] is presented in Fig. 8. Again, the dark center of rosettes is aligned with the bright rows as sketched in Fig. 3. Where rosettes connect to strands, the fourfold-coordinated Ti atom and one of the supporting O atoms have been removed as discussed above. The rosette (i) and ring (ii) share two common two fivefold-coordinated Ti atoms above the bridging O atoms of the  $(1 \times 1)$  substrate. Both structures are one  $(1 \times 1)$  unit cell wide in the  $[1\bar{1}0]$  direction. The large ring (iii) is boarded by  $\text{Ti}_2\text{O}_3$  rows, which are

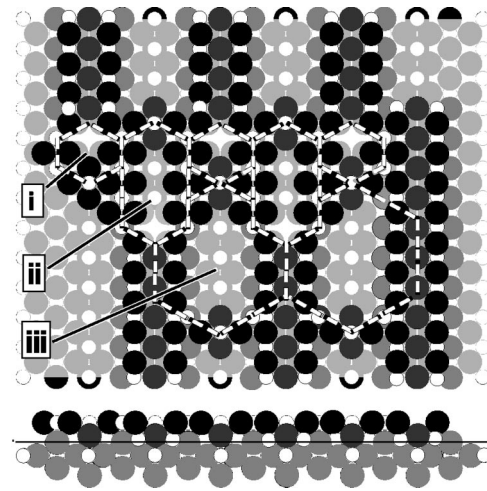


FIG. 8. Atomic model (top and side view) for a reconstructed  $\text{TiO}_2(110)$  surface after annealing in UHV composed of (i) rosettes, (ii) rings, and (iii) larger rings. Large black balls and small white balls correspond to oxygen and titanium atoms, respectively.

separated by two  $(1 \times 1)$  unit cells. At the bottom, large rings are linked to form the zigzag-shaped chains, which can be recognized in Fig. 6.

This atomic model is a logical outgrowth of the atomic model for the strands connected to rosettes presented in Fig. 3. Because the cross-linked strands evolve from the rosette network, it is natural to assume the same building blocks for both structures. Attempts to construct atomic models for cross-linked strands with large and small rings using either the single-chain model [Fig. 3(i)] or the added-row model of Pang *et al.* [Fig. 3(ii)] resulted in far less satisfactory agreement with our STM data.

Interestingly, Bennett *et al.* report cross-linked strands that were interpreted as  $\text{Ti}_3\text{O}_5$  strands (with extra bridging oxygen atoms) connected by cross shapes structurally similar to rosettes. These have been produced by annealing in oxygen at 870 K.<sup>16</sup> The presence of one or the other  $(1 \times 2)$  reconstruction appears to be dependent on the reduction state of the  $\text{TiO}_2$  crystal;  $(1 \times 2)$  strands consistent with the Onishi-Iwasawa model were observed on more stoichiometric crystals.<sup>16</sup> For the crystal (blue) used in our experiment, only the latter type of  $(1 \times 2)$  strands was observed. One reason for this discrepancy could be that our STM experiment was made at room temperature. The cooling of the crystal in our experimental setup is very slow, and the quenching process might affect the surface structure. In addition, the reduction state of the crystal has a great influence on the surface morphology evolving at elevated temperatures in UHV as well as in an oxygen environment.<sup>7,19</sup> Possibly, different reduction states of crystals used by various groups could give rise to the different validity of models for cross-linked  $(1 \times 2)$  strands.

### C. Mechanism

As discussed in detail in our previous paper<sup>7</sup> and by others<sup>16,20,26</sup> the main features on the oxygen-restructured  $\text{TiO}_2(110)$  surfaces are created by reaction of gaseous oxygen with interstitial  $\text{Ti}^{3+}$  ions segregating from the reduced bulk towards the surface. At temperatures between 500 and

710 K, all three features [rosettes,  $(1 \times 2)$  strands, and  $(1 \times 1)$  islands] are seen. Above 710 K, only strands and islands are formed. Exposure to oxygen above 830 K renders large  $(1 \times 1)$  terraces.

UHV annealing a restructured surface at 620 K flattens the surface, but the rosette networks still survive as shown in Fig. 4. Above 690 K [Fig. 5(b)], the surface morphology undergoes a dramatic change as follows: network +  $(1 \times 1)$  islands +  $(1 \times 2)$  strands  $\rightarrow$   $(1 \times 2)$  strands +  $(1 \times 1)$  terraces (780 K)  $\rightarrow$   $(1 \times 1)$  terraces (830 K). In the STM images of Figs. 5(a) and 5(b), the number of rosette network patches decreases dramatically, and a high concentration of  $(1 \times 2)$  strands appears. The surface morphology changes in the high-temperature range (above 710 K) of UHV annealing are similar to those of the  $\text{Ti}^{18}\text{O}_2$  surface under oxygen environment at high temperature.<sup>7</sup> This suggests that the dominating mechanisms for the phase transition during annealing at high temperature could be the same in both UHV and oxygen surroundings.

Three possible mechanisms may cause the surface morphology change at elevated temperatures. First,  $\text{TiO}_2$  units may detach from rosettes or from  $(1 \times 2)$  strands, diffuse across the surface, and incorporate into  $(1 \times 1)$  islands. Second, additional Ti and O atoms from the substrate may diffuse to the surface and convert rosettes into  $(1 \times 1)$  islands by filling empty sites such as the centers of rosettes. Third, both rosettes and  $(1 \times 2)$  strands may decompose with oxygen desorbing into the vacuum and Ti cations diffusing into the bulk, which is just the opposite process of oxygen-induced restructuring.<sup>7</sup> All three processes could occur simultaneously with different rates in different temperature regimes. Only processes two and three will result in a change of surface composition, while process one involves a mere rearrangement of surface atoms.

UHV annealing of oxygen-restructured surfaces decreases the  $^{18}\text{O}$  surface content. In Fig. 7, a clear break point is visible at 740 K with slower depletion of  $^{18}\text{O}$  in region I ( $<740$  K) and a much faster rate above this temperature (region II). Region I corresponds to the disappearance of most rosette networks, with only a few cross-links of  $(1 \times 2)$  strands surviving [Figs. 5(a) and 5(b)]. The temperature regime of region II starts between Figs. 5(b) and 5(c) where  $(1 \times 2)$  strands convert into the  $(1 \times 1)$  surface. Henderson<sup>30</sup> has studied bulk-assisted oxidation of reduced  $\text{TiO}_2$  surfaces (which were produced by both sputtering and deposition of excess Ti) and has observed a drastic change in the rate of diffusion mechanisms at a similar temperature. The slight increase in the O:Ti ratio below  $\sim 700$  K was explained by exchange of Ti and O within the reduced region. Above 700 K, excess Ti starts to diffuse into the bulk, which leads to a rapid reoxidation of the surface. Interestingly, the rate of  $^{18}\text{O}$  decrease/ $^{16}\text{O}$  increase was faster in the

low-temperature regime of Henderson's static secondary ion mass spectrometry experiment,<sup>30</sup> which was interpreted as diffusion of O in the sputtered film.

Henderson's results are consistent with the behavior observed in this work. The exchange of  $^{18}\text{O}$  with bulk  $^{16}\text{O}$  (second process: near surface  $\text{TiO}_2$  or O moves upward and fills the centers of rosettes) dominates at lower temperatures below 740 K. This process is relatively slow. Region II corresponds to the disappearance of  $\text{Ti}_2\text{O}_3$  strands. Probably this occurs via process three,  $^{18}\text{O}$  desorption into the gas phase, which happens faster and gives rise to the rapid reduction of the  $^{18}\text{O}$  surface content. The desorption of oxygen from the surface is supported by creation of oxygen defects<sup>31</sup> above 700 K and the Xu *et al.* STM study on the creation of a  $(1 \times 2)$  reconstructed surface above 700 K.<sup>14</sup> The oxygen desorption process is accompanied by diffusion of excess Ti into the bulk. At any given temperature, massive surface diffusion (first process) leads to an overall increase of terrace size.

## V. SUMMARY

UHV annealing of oxygen-restructured  $\text{Ti}^{18}\text{O}_2(110)$  surfaces (prepared by annealing in  $^{18}\text{O}_2$  at 550 K) causes a dramatic surface morphology change. The "rough" surface characterized by three main elements [rosette networks,  $(1 \times 2)$  strands, and  $(1 \times 1)$  islands] is smoothed with elevated annealing temperatures through the conversion of metastable rosette networks to  $(1 \times 2)$  strands and finally to stable  $(1 \times 1)$  terraces. A depletion of surface  $^{18}\text{O}$  occurs concurrent with the morphology change. The main results are summarized as follows.

(1) For the  $(1 \times 2)$  strands, an induced added-row  $\text{Ti}_2\text{O}_3$  structure is favored by atomically resolved STM measurements of oxygen-annealed surfaces and of cross-linked  $(1 \times 2)$  strands obtained by UHV annealing.

(2) The smoothing process on oxygen-restructured  $\text{TiO}_2(110)$  surfaces depends on annealing temperature. Rosette network patches disappear above 690 K.  $(1 \times 2)$  strands and  $(1 \times 1)$  islands exist up to 830 K. Above 830 K, only large, flat  $(1 \times 1)$  terraces exist.

(3) Two different temperature regimes are observed. Below 740 K, depletion of  $^{18}\text{O}$  occurs relatively slowly. This is attributed to diffusion of mainly oxygen leading to an  $^{16}\text{O}/^{18}\text{O}$  exchange with the bulk. Above 740 K, desorption of oxygen into the gas phase and diffusion of excess Ti into the bulk cause a more rapid decrease of the surface oxygen content.

## ACKNOWLEDGMENTS

This work was supported in part by NSF-CAREER and DoE-EPSCoR. The help of Dr. Lanping Zhang with data taking and useful discussions with Dr. Michael A. Henderson are gratefully acknowledged.

\*Author to whom correspondence should be addressed. Fax: +1 504 862 8702. Electronic address: diebold@mailhost.tcs.tulane.edu

<sup>1</sup>B. L. Maschhoff, J.-M. Pan, and T. E. Madey, *Surf. Sci.* **259**, 190 (1991).

<sup>2</sup>G. Charlton, P. B. Howes, C. L. Nicklin, P. Steadman, J. S. G. Taylor, C. A. Muryn, S. P. Hartre, J. Mercer, R. McGrath, D.

Norman, T. S. Turner, and G. Thornton, *Phys. Rev. Lett.* **78**, 495 (1997).

<sup>3</sup>B. Hird and R. A. Armstrong, *Surf. Sci.* **420**, L131 (1999).

<sup>4</sup>M. Ramamoorthy, D. Vanderbilt, and R. D. King-Smith, *Phys. Rev. B* **49**, 16 721 (1994).

<sup>5</sup>M. Li, W. Hebenstreit, and U. Diebold, *Surf. Sci. Lett.* **414**, L951 (1998).

- <sup>6</sup>M. Li, W. Hebenstreit, U. Diebold, M. A. Henderson, and D. R. Jennison, *Faraday Discuss.* (to be published).
- <sup>7</sup>M. Li, W. Hebenstreit, L. Gross, U. Diebold, M. A. Henderson, D. R. Jennison, P. A. Schultz, and M. P. Sears, *Surf. Sci.* **437**, 173 (1999).
- <sup>8</sup>P. J. Møller and M.-C. Wu, *Surf. Sci.* **224**, 265 (1989).
- <sup>9</sup>D. Novak, E. Garfunkel, and T. Gustafsson, *Phys. Rev. B* **50**, 5000 (1994).
- <sup>10</sup>H. Onishi and Y. Iwasawa, *Surf. Sci. Lett.* **313**, 783 (1994).
- <sup>11</sup>M. Sander and T. Engel, *Surf. Sci. Lett.* **302**, 263 (1994).
- <sup>12</sup>P. W. Murray, N. G. Condon, and G. Thornton, *Phys. Rev. B* **51**, 10 989 (1995).
- <sup>13</sup>A. Berkó and F. Solymosi, *Langmuir* **12**, 1257 (1996).
- <sup>14</sup>C. Xu, X. Lai, G. W. Zajac, and D. W. Goodman, *Phys. Rev. B* **56**, 13 464 (1997).
- <sup>15</sup>R. E. Tanner, M. R. Castell, and G. A. D. Briggs, *Surf. Sci.* **412/413**, 672 (1998).
- <sup>16</sup>R. A. Bennett, P. Stone, N. J. Price, and M. Bowker, *Phys. Rev. Lett.* **82**, 3831 (1999).
- <sup>17</sup>C. L. Pang, S. A. Haycock, H. Raza, P. W. Murray, and G. Thornton, *Phys. Rev. B* **58**, 1586 (1998).
- <sup>18</sup>S. Fischer, A. W. Munz, K.-D. Schierbaum, and W. Göpel, *Surf. Sci.* **337**, 17 (1995).
- <sup>19</sup>M. Li, W. Hebenstreit, U. Diebold, A. M. Tyryshkin, M. K. Bowman, G. G. Dunham, and M. A. Henderson, *J. Phys. Chem.* (to be published).
- <sup>20</sup>P. Stone, R. A. Bennett, and M. Bowker, *New J. Phys.* **1**, 1 (1999).
- <sup>21</sup>A. Szabo and T. Engel, *Surf. Sci.* **329**, 241 (1995).
- <sup>22</sup>U. Diebold, J. F. Anderson, K.-O. Ng, and D. Vanderbilt, *Phys. Rev. Lett.* **77**, 1322 (1996).
- <sup>23</sup>O. Gülseren, R. James, and D. W. Bullett, *Surf. Sci.* **377-379**, 150 (1997).
- <sup>24</sup>K.-O. Ng and D. Vanderbilt, *Phys. Rev. B* **56**, 10 544 (1997).
- <sup>25</sup>Q. Guo, I. Cocks, and E. M. Williams, *Phys. Rev. Lett.* **77**, 3851 (1996).
- <sup>26</sup>H. Onishi, and Y. Iwasawa, *Phys. Rev. Lett.* **76**, 791 (1996).
- <sup>27</sup>L. Zhang, M. Kuhn, and U. Diebold, *Surf. Sci.* **371**, 223 (1997).
- <sup>28</sup>H. Onishi, K. Fukui, and Y. Iwasawa, *Bull. Chem. Soc. Jpn.* **68**, 2447 (1995).
- <sup>29</sup>M. Aono and R. R. Hasiguti, *Phys. Rev. B* **48**, 12 406 (1993).
- <sup>30</sup>M. A. Henderson, *Surf. Sci.* **419**, 174 (1999).
- <sup>31</sup>J.-M. Pan, B. L. Maschhoff, U. Diebold, and T. E. Madey, *J. Vac. Sci. Technol. A* **10**, 2470 (1992).